RSC Advances

PAPER

View Article Online
View Journal | View Issue

Check for updates

Cite this: *RSC Adv.*, 2017, **7**, 34425

Kinetics of phosphine substitution in $CpRu(PPh_3)_2X$ (X = Cl, Br, I, N_3, and NCO)†

David Hill,[a] Connor Delaney,[a] Miles Clark,[a] Mathew Eaton,[a] Bakar Hassan,[a] Olivia Hendricks,[b] Duy Khoi Dang[a] and Rein U. Kirss *[a]

The kinetics of phosphine substitution in $CpRu(PPh_3)_2X$ (X = Br, **1b**, X = I, **1c**, X = N_3, **1d**, and X = NCO, **1e**) have been measured under pseudo-first order conditions in THF solution and compared with data for $CpRu(PPh_3)_2X$ (**1a**). The relative rate of substitution is found to be **1a** > **1d** > **1b** > **1e** > **1c**. Substitution rates decrease in the presence of added PPh_3 and are independent of added X consistent with a dissociative process. Activation parameters for **1a–1c** ($\Delta H^{\dagger}$ = 113–135 kJ mol^{-1}, $\Delta S^{\dagger}$ = 21–102 J mol^{-1} K^{-1}) and DFT calculations support a dissociative or dissociative interchange pathway even though negative activation entropies ($\Delta S^{\dagger}$ = −48 ± 16 to −105 ± 5 J mol^{-1} K^{-1}) are observed for **1d–e**. Differences in Ru–ligand bond angles in **1d–e** point to different π-acceptor properties of the pseudohalide ligands, contributing to the faster rate of substitution for the azide complexes, **1d** relative to the cyanate derivative **1e**. Substitution is not observed when X = F, **1f**, X = H, **1g**, X = SnF_3, **1h**, or X = $SnCl_3$, **1i**. Compounds **1b–1e** also react with chloroform to yield **1a**. The rates of halide exchange are comparable to phosphine substitution for **1c** and **1d**. The latter reaction is inhibited by excess triphenylphosphine and is unaffected by both radical inhibitors and radical traps suggesting that a radical mechanism is unlikely.

Received 7th March 2017
Accepted 15th June 2017

DOI: 10.1039/c7ra02793a

rsc.li/rsc-advances

Open Access Article. Published on 07 July 2017. Downloaded on 2/5/2026 2:55:27 PM.
This article is licensed under a Creative Commons Attribution 3.0 Unported Licence.

Introduction

Cyclopentadienyl ruthenium bis(triphenylphosphine) chloride, $CpRu(PPh_3)_2Cl$ (**1a**), is a versatile catalyst for a range of useful transformations.[1] Changing the halide ligand in $CpRu(PPh_3)_2Cl$ for other halides or pseudohalides affects both the reactivity and selectivity in these processes.[2] For example, $CpRu(PPh_3)_2I$ (generated *in situ*) is reported to be more effective than $CpRu(PPh_3)_2Cl$ in catalyzing the cycloaddition of norbornene and norbornadiene.[3] A mechanism based on faster phosphine dissociation is proposed as the explanation for the increased catalytic activity of $CpRu(PPh_3)_2I$. On the other hand, $CpRu(PPh_3)_2X$ catalyzed conversion of cyclohexylamine and methanol to $CyNMe_2$ is nearly quantitative after 6 hours at 100 °C for X = Cl while only 40% conversion to 2.4 : 2.8 : 1 ratio of cyclohexylimine, methylcyclohexylamine and $CyNMe_2$ is observed for X = I.[4] In this case, the ionization of the Ru–X bond is proposed as the key step the reaction mechanism. The conversion rate of methanol to methyl acetate in the presence of catalytic amounts of $CpRu(PPh_3)_2X$ (X = F, Cl, Br, SnF_3, $SnCl_3$ and $SnBr_3$) follows the order: X = SnF_3 > $SnCl_3$ ≈ $SnBr_3$ > F > Cl ≈ Br.[5] In this case, dissociation of chloride is thought to be counterproductive to efficient catalysis with the greater activity of $CpRu(PPh_3)_2SnF_3$ attributed to phosphine dissociation. The kinetics of phosphine substitution in $CpRu(PAr_3)_2Cl$[6,7] and the rate of solvolysis of the halide in $CpRu(PR_2R')_2X$ (R = Ph, Me, X = Cl, Br, I)[8] have both been measured but the effect of X on the rate of phosphine substitution (eqn (1)) has not been extensively explored. Only for the related $Cp^*Ru(PMe_3)_2X$[9] has the effect of the ancillary X ligand on the rate of phosphine substitution been systematically investigated. The data for the latter were consistent with a dissociative mechanism with a marked increase in rate for better π-donor X ligands. In the present study we report on the phosphine substitution in $CpRu(PPh_3)_2X$ (eqn (1), **1b–i** where X = Br, I, N_3, NCO, H, F, $SnCl_3$, and SnF_3) in THF as well as on the unexpected halide exchange reaction between **1b–e** and $CDCl_3$. The results provide some insight into the relative importance of Ru–P dissociation in catalytic reactions involving **1a–i**.

Experimental

All compounds described in this work were handled using Schlenk techniques or a M. I. Braun glove box under purified nitrogen atmospheres.[10] $RuCl_3 \cdot xH_2O$ was purchased from Pressure Chemical, Inc. Tertiary phosphines, $PMePh_2$ and PPh_3, were obtained from Strem Chemical, Inc. and used as

[a]Department of Chemistry and Chemical Biology, Northeastern University, Boston, MA 02115, USA. E-mail: r.kirss@neu.edu

[b]Department of Chemistry, Wellesley College, Wellesley, MA 02481, USA

† Electronic supplementary information (ESI) available: Representative plots ln [$CpRu(PPh_3)_2X$] *vs.* *t* for phosphine substitution and halide exchange, Eyring plots, and coordinates for the optimized geometries for **1a–e**. See DOI: 10.1039/c7ra02793a

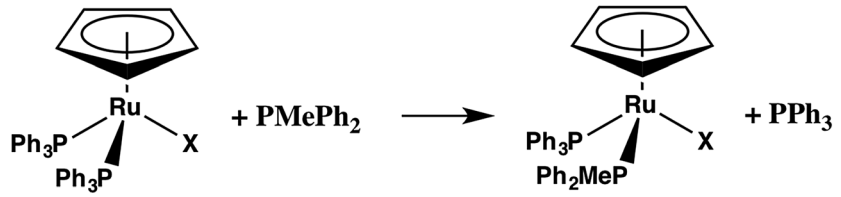

(1)

1a. X = Cl **f.** X = F
b. = Br **g.** = H
c. = I **h.** = SnF_3
d. = N_3 **i.** = $SnCl_3$
e. = NCO

2a. X = Cl
b. = Br
c. = I
d. = N_3
e. = NCO

Open Access Article. Published on 07 July 2017. Downloaded on 2/5/2026 2:55:27 PM.
This article is licensed under a Creative Commons Attribution 3.0 Unported Licence.

received. Solvents were purified by refluxing over Na/benzophenone (toluene, tetrahydrofuran, benzene, hexane, pentane), P_2O_5 (dichloromethane) or $MgSO_4$ (ethanol) and distilled prior to use. Chloroform-d^1 and benzene-d^6 (Cambridge Isotope Laboratories) were purified by distillation from CaH_2 and Na/benzophenone, respectively. Ruthenium(II) compounds $CpRu(PPh_3)_2Cl$ (**1a**),[11] $CpRu(PPh_3)_2Br$ (**1b**),[12] $CpRu(PPh_3)_2I$ (**1c**),[12] $CpRu(PPh_3)_2N_3$ (**1d**),[13] $CpRu(PPh_3)_2NCO$ (**1e**),[12] $CpRu(PPh_3)_2H$ (**1f**),[12] $CpRu(PPh_3)_2F$ (**1g**),[14] $CpRu(PPh_3)_2SnF_3$ (**1h**),[13] $CpRu(PPh_3)_2SnCl_3$ (**1i**),[13] and $CpRu(PPh_3)(PPh_2Me)Cl$ (**2a**),[15] were prepared by literature procedures. Melting points were determined in capillary tubes using an Electrothermal 9110 melting point apparatus and are uncorrected. Elemental analyses (C, H) were performed by Columbia Analytical Services, Inc. Tucson, AZ.

NMR spectra were recorded at 400 MHz for ^1H and 162 MHz for $^{31}P\{^1H\}$ on a Mercury XL300 spectrometer. Proton chemical shifts are reported relative to residual protons in the solvent ($CD_2\mathbf{H}Cl$ at δ 7.24 ppm relative to TMS at 0.00 ppm). Phosphorus chemical shifts are reported relative to 85% $H_3\mathbf{P}O_4$ at 0.0 ppm.

Electrochemical measurements were made under nitrogen on a BAS 100 B/W electrochemical workstation at 22 °C using 1×10^{-3} M solutions in dry CH_2Cl_2, 0.1 M $^nBu_4NPF_6$ as supporting electrolyte at a scan rate of 100 mV s^{-1}. The working electrode was a 3 mm Pt disk with a Pt wire as auxiliary electrode. A silver wire was used as a pseudo-reference electrode with ferrocene added as an internal standard. All potentials for **1a–e**, **h** and **i** (Table 1) are referenced to ferrocene ($E_{1/2} = 0.00$ V).

Table 1 Electrochemical potentials for selected $CpRu(PPh_3)_2X$ complexes[a]

Compound	E° (mV)	Compound	E° (mV)
X = Cl, **1a**	136	X = NCO, **1e**	168
X = Br, **1b**	138	X = F, **1g**	790
X = I, **1c**	182	X = SnF_3, **1h**	[b]
X = N_3, **1d**	20	X = $SnCl_3$, **1i**	730

[a] 1×10^{-3} M solutions in dry CH_2Cl_2, 0.1 M $^nBu_4NPF_6$ as supporting electrolyte at a scan rate of 100 mV s^{-1} at 22 °C *vs.* Fc/Fc^+ at 0.00 mV. [b] **1h** is not sufficiently soluble for the experiment.

Synthesis of $CpRu(PPh_3)(PMePh_2)X$ (X = Br, I, NCO, N_3, SCN, and $SnCl_3$)

General procedure. A slurry of $CpRu(PPh_3)(PMePh_2)$ Cl (**2a**) and a 5–10 fold excess of KX (X = Br, I, N_3, NCO, SCN) was refluxed in 25 mL absolute ethanol for 16–18 h under nitrogen. Solvent was evaporated under vacuum and the product extracted with 2×25 mL CH_2Cl_2. After filtration to remove the potassium salts, the filtrate was evaporated to dryness and the crude product crystallized from CH_2Cl_2/hexane to yield $CpRu(PPh_3)_2X$ (**1b–f**). Chromatography on neutral alumina with dichloromethane served as an additional purification method.

*$CpRu(PPh_3)(PMePh_2)Br$ (**2b**).* Yellow-orange solid, 75% yield. Mp turns dark brown without melting above 160 °C.

Calculated for $C_{36}H_{33}P_2RuBr\cdot CH_2Cl_2$: 56.01% C, 4.45% H; found: 56.53% C, 5.35% H.

^1H ($CDCl_3$) δ 1.19 d (J = 8.8 Hz, 3H, PCH_3), 4.20 s (5H, Cp), 5.29 s (2H, CH_2Cl_2), 7.0–7.8 m (25 H, aryl).

^{31}P ($CDCl_3$) δ 42.9 d (J_{PP} = 43 Hz), 29.9 d (J_{PP} = 43 Hz).

*$CpRu(PPh_3)(PMePh_2)I$ (**2c**).* Yellow-orange solid, 51% yield. Mp turns dark brown without melting above 140 °C.

Calculated for $C_{36}H_{33}P_2RuI\cdot CH_2Cl_2$: 52.87% C, 4.20% H; found: 53.08% C, 4.67% H.

^1H ($CDCl_3$) δ 1.31 d (J = 8.8 Hz, 3H, PCH_3), 4.27 s (5H, Cp), 5.24 s (2H, CH_2Cl_2), 7.0–7.8 m (25 H, aryl).

^{31}P ($CDCl_3$) δ 42.9 d (J_{PP} = 43 Hz), 30.0 d (J_{PP} = 43 Hz).

*$CpRu(PPh_3)(PMePh_2)N_3$ (**2d**).* Yellow-orange solid, 15% yield. Mp turns dark brown without melting above 163 °C.

Calculated for $C_{36}H_{33}N_3P_2Ru$: 64.47% C, 4.96% H; found: 63.93% C, 5.31% H.

^1H ($CDCl_3$) δ 1.17 d (J = 8.8 Hz, 3H, PCH_3), 4.23 s (5H, Cp), 7.21–7.46 m (25 H, aryl).

^{31}P ($CDCl_3$) δ 41.3 d (J_{PP} = 43 Hz), 30.3 d (J_{PP} = 43 Hz).

*$CpRu(PPh_3)(PMePh_2)NCO$ (**2e**).* Yellow-orange solid, 74% yield. Mp turns black without melting above 160 °C.

Calculated for $C_{37}H_{33}NOP_2Ru$: 66.26% C, 4.96% H; found: 66.45% C, 5.28% H.

^1H ($CDCl_3$) δ 1.06 d (J = 8.8 Hz, 3H, PCH_3), 4.15 s (5H, Cp), 7.18–7.3 m (25 H, aryl).

^{31}P ($CDCl_3$) δ 39.5 d (J_{PP} = 43 Hz), 30.7 d (J_{PP} = 42 Hz).

*$CpRu(PPh_3)(PMePh_2)SnCl_3$ (**2i**).* A solution of 172 mg (0.26 mmol) **2a** and 54 mg (0.28 mmol) $SnCl_2$ in 50 mL absolute ethanol was refluxed for 90 minutes. The resulting precipitate was isolated

 This journal is © The Royal Society of Chemistry 2017

Open Access Article. Published on 07 July 2017. Downloaded on 2/5/2026 2:55:27 PM.
This article is licensed under a Creative Commons Attribution 3.0 Unported Licence.

by filtration, washed 2 × 5 mL methanol and dried under vacuum. Compound **2i** was isolated in 68% yield as an orange solid. Mp. turns dark brown without melting 151–153 °C.

Calculated for $C_{36}H_{33}P_2RuSnCl_3$: 50.65% C, 3.90% H; found: 50.83% C, 4.54% H.

^{1}H ($CDCl_3$) δ 1.19 d (J = 8.8 Hz, 3H, PCH_3), 4.19 s (5H, Cp), 6.9–7.7 m (28 H, aryl).

^{31}P ($CDCl_3$) δ 43.4 d (J_{PP} = 44 Hz), 30.4 d (J_{PP} = 44 Hz).

Kinetic measurements

Reactions of 1b–e with $PMePh_2$. The collection of kinetic data for reactions between **1b–e** with $PMePh_2$ followed procedures described for reactions between $CpRu(PAr_3)_2Cl$ and $PMePh_2$.[6] Stock solutions of **1b–e** (10.0 mL) were prepared in volumetric flasks by dissolving an appropriate amount of **1b–e** and a 10–15 fold excess of $PMePh_2$ in $CDCl_3$ or THF containing 10% C_6D_6. Samples for the kinetic experiments were prepared by transferring 600 μL of the stock solution to 5 mm NMR tubes attached to 14/20 ground glass joints. The tubes were flame-sealed sealed under vacuum. Samples were stored at −20 °C until needed and then heated in thermostated block heaters. The rate of substitution of PPh_3 by PMe_2Ph was measured by monitoring the decrease in the singlet for $CpRu(PPh_3)_2X$ (**1b–e**) over time relative to the doublets for $CpRu(PPh_3)(PMePh_2)X$ (**2b–e**). Three independent measurements of the substitution rate were made at each temperature to determine the rate constants for the reaction.

To assess the effect of excess PPh_3 and X^-, additional experiments were carried out by adding 600 μL of the stock solution to weighed amounts of PPh_3 (3–10 equivalents) or ^{n}Bu$_4$NX (≈10 equivalents). The resulting solutions were transferred to NMR tubes and sealed as described above. These experiments were typically limited to a single measurement of the substitution rate at one temperature.

Activation parameters were determined using the Eyring equation by plotting $\ln(k_{obs}/T)$ *vs.* $1/T$ where the slope $= -\Delta H^{\ddagger}/R$ and the intercept $= \Delta S^{\ddagger}/R + \ln k_B/h$ as described in our prior work.[6] The activation entropies and enthalpies were also calculated from the slope and intercept of a plot of $T\ln(k/T)$ *vs.* T, respectively.[16] The same values for $\Delta H^{\ddagger}$ and $\Delta S^{\ddagger}$ were obtained using each method within error. Errors in $\Delta S^{\ddagger}$ and $\Delta H^{\ddagger}$ were calculated using the statistical packages in Excel and by procedures described in standard analytical chemistry texts.[17]

Reactions of 1c–d with $CDCl_3$. Flame sealed tubes containing 10–15 mM solutions of **1c–d** were prepared as described for the reactions with $PMePh_2$. The rate of the halide exchange reaction was determined by integration of the singlets assigned to **1a** and **1c–d** in the ^{31}P NMR spectra. Additional tubes containing PPh_3 (6–21 eq.), 9,10-dihydroanthraene (3–16 eq.) and duroquinone (2–24 eq.) were prepared by adding 600 μL of the stock solution to weighed amounts of these reagents.

Computational methods

All calculations were conducted using density functional theory (DFT) as implemented in the Gaussian09 Revision B.01 suite of *ab initio* quantum chemistry programs as described for phosphine substitution in **1a** and related $CpRu(PAr_3)_2Cl$ complexes.[6]

Results

Kinetics of phosphine exchange

The substitution of one PPh_3 in **1b–e** by PPh_2Me (10–15 equivalents, pseudo first order conditions) was followed by ^{31}P NMR in both $CDCl_3$ and THF/10% C_6D_6 (v/v) solution between 25 and 60 °C. The singlet resonance for the starting material is replaced by a pair of doublets assigned to the mono-substituted products, $CpRu(PPh_3)(PPh_2Me)X$ (**2b–e**) with concurrent appearance of resonances for PPh_3 (δ − 4.4 ppm in $CDCl_3$, −4.6 ppm in THF/10% C_6D_6). The ^{31}P chemical shifts of the products were verified by comparison with independently synthesized and characterized samples of **2b–f**. Formation of $CpRu(PPh_2Me)_2X$ (*i.e.* di-substitution) is not observed during the reaction period even in the presence of ≈10 equivalents of $PMePh_2$. Formation of **1b–c** from reactions between **2b–c** and PPh_3 is not observed. Qualitatively, the rate of reaction at 40 °C is found to be **1a** > **1d** > **1b** ≈ **1e** > **1c**.

Reactions between $CpRu(PPh_3)_2X$ and $PMePh_2$ in THF solution follow first order kinetics over several half-lives. Rate constants, half-lives and activation parameters for reactions in THF/C_6D_6 mixtures are summarized in Fig. 1 and Table 2. The reaction rates are largely independent of the [$PMePh_2$], up to 60 equivalents (Fig. 2 and Table S3†). By comparison, the reaction rate decreases dramatically in the presence of added PPh_3. In addition, the reaction rates are unaffected by the addition of excess ^{n}Bu$_4$NX in all four cases.[18] The rates of phosphine substitution in **1a** in both $CDCl_3$ and in THF are known.[6,7] The remaining complexes, **1f–g** and **1i** fail to react with excess $PMePh_2$ in THF/C_6D_6, dioxane/C_6D_6 or other solvent mixtures up to the boiling point of the solvents even after 30 days or more. Compound **1h** has minimal solubility in THF and dioxane hampering comparable studies, however, phosphine substitution was not observed.

The activation parameters reveal different trends for the halide complexes **1a–c** and the pseudohalide complexes **1d–e**. Activation enthalpies for the former are generally larger and the activation entropies are positive. The activation entropies for **1d** and **1e**, however, are negative. The free energies of activation ($\Delta G^{\ddagger}$) calculated at 25 °C (298 K) for **1a–e** are similar

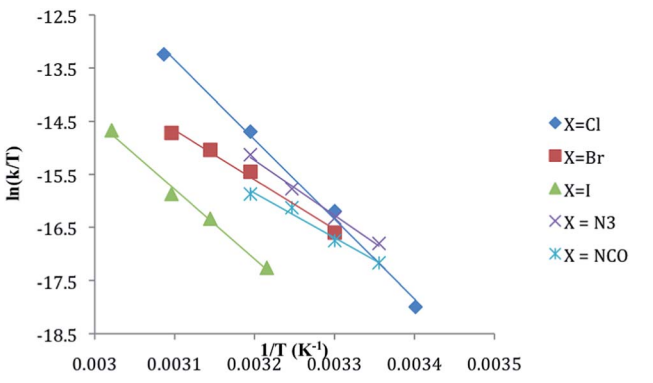

Fig. 1 Eyring plots of $\ln(k_{obs}/T)$ *vs.* $1/T$ for **1b–e** in THF containing 10% v/v C_6D_6.

Open Access Article. Published on 07 July 2017. Downloaded on 2/5/2026 2:55:27 PM.
This article is licensed under a Creative Commons Attribution 3.0 Unported Licence.

Table 2 Rate constants, half-lives, and activation parameters for the substitution of PPh_3 by $PMePh_2$ in **1a–e** in THF containing 10% (v/v) C_6D_6[a]

X	$k_{30,THF}$ ($\times 10^6$ s^{-1})	$t_{1/2}$ (h)	$\Delta H^{\ddagger}$ (kJ mol^{-1})	$\Delta S^{\ddagger}$ (J mol^{-1} K^{-1})	$\Delta G^{\ddagger}$ (kJ mol^{-1})
1a, Cl^-	29 ± 2[b]	0.66	121 ± 4[b]	71 ± 8[b]	100
1b, Br^-	7.89 ± 0.79	24	135 ± 7	102 ± 23	105
1c, I^-	2.49 ± 0.3	77	113 ± 4	21 ± 12	107
1d, N_3^-	24.6 ± 1.5	7.8	86 ± 5	−48 ± 16	100
1e, NCO^-	16.1 ± 3.6	12	70 ± 7	−105 ± 23	101

[a] Concentrations of **1b–e** ranged from 8 to 17 mM with $a \approx$ 10–15 fold excess of $PMePh_2$. Benzene-d^6 is added to lock and shim the spectrometer. [b] From ref. 7.

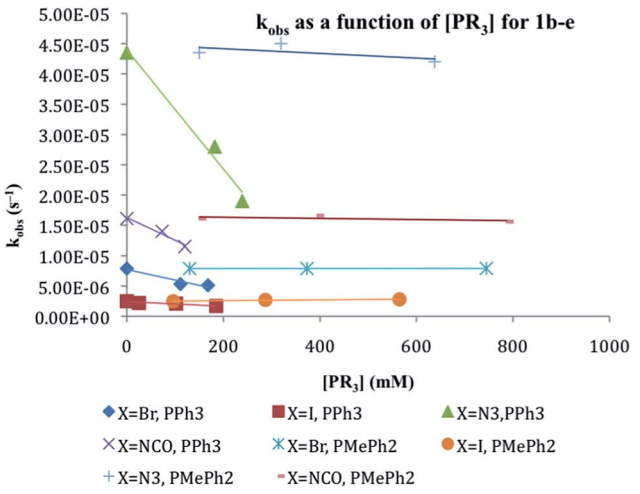

Fig. 2 Plots of k_{obs} as a function of [$PMePh_2$] and [PPh_3] for the reaction between $CpRu(PPh_3)_2X$ (**1b–e**) and excess $PMePh_2$ in THF. The data are for reactions at 30 °C except for X = N_3 (**1d**) which was collected at 35 °C.

to those reported for $Cp^*Ru(PMe_3)_2X$: 109 kJ mol^{-1}, 106 kJ mol^{-1} and 113 kJ mol^{-1} for X = Cl, Br, and I, respectively.[9] Pseudohalide derivatives in the $Cp^*Ru(PMe_3)_2X$ series were not studied.

Reactions between **1b–e** and $PMePh_2$ were also investigated in $CDCl_3$ but were complicated by the appearance of **1a** (δ 39.9 ppm) and **2a** as the reaction progressed. The formation of **1a** is the result of reaction between the starting materials and the solvent since the starting materials were pure by ^{31}P NMR at the outset of the reaction. Thus the final reaction mixtures in $CDCl_3$ contain **2b–e** and **2a**. Nevertheless, the rate of reaction between excess $PMePh_2$ (10–15 equivalents, *i.e.* pseudo first order conditions in $PMePh_2$) and **1b–e** at early reactions times could be measured by integration of the ^{31}P resonances for reactant and product before halide exchange led to measurable quantities of **1a**. Qualitatively, the order of the rates for the reaction of **1b–e** with $PMePh_2$ in $CDCl_3$ is the same as in THF: **1a** > **1d** > **1b** > **1e** > **1c**. Reasonable estimates of first order rate constants ($k_{subs,CDCl_3}$) for the substitution reactions in $CDCl_3$ at early reaction times, when less than 5% of **1a** (and no **2a**) is observed in the solution, are summarized in Table 3. The substitution is slowed by the addition of excess PPh_3 and the formation of **1a** in these reactions is suppressed in the presence of added $^nBu_4NX$. The rate of substitution, however, remains unaffected by the presence of excess X^-. Comparison of the values for $k_{subs,THF}$ with $k_{subs,CDCl_3}$ for **1a–e** indicate that reactions are between 1.5 and 5 times faster in THF solution.

Kinetics of halide exchange between 1c–d and $CDCl_3$

The rates of the halide exchange reactions between **1c** and **1d** with $CDCl_3$ were measured independently by integration of the ^{31}P resonances for reactants (**1c–d**) and product (**1a**) in $CDCl_3$ at 30 °C. Linear plots of ln[$CpRu(PPh_3)_2X$] *vs.* time are observed for both compounds, with first order rate constants for the reaction (k_{CDCl_3}) being listed in Table 3. The rate of reaction with $CDCl_3$ reflects the same order observed for phosphine substitution: **1d** > **1c**. The reaction rates of **1c–d** in $CDCl_3$ were further investigated in the presence of excess PPh_3, (6–21 eq.), a radical initiator, 9,10-dihydroanthracene, (3–16 eq.), and a radical trap, duroquinone, (2–24 eq.). Fig. 3 reveals that the reaction rates are essentially independent of radical initiators and traps but are slowed significantly by the presence of PPh_3. The $k_{subs,CDCl_3}/k_{CDCl_3}$ ratio in Table 3 reveals that the rate of reaction with $CDCl_3$ is competitive with the rate of phosphine substitution for **1c–d**.

Computational studies

DFT calculations were initially used to optimize the structures of **1a–e** (Table 4). The calculated values for bond distances and bond angles for **1a–b** and **1d** compare favorably with the published structures determined by X-ray crystallography: the calculated bond distances are only slightly longer than the observed values.[19]

Computational chemistry was then applied to the calculation of the relative energies of potential intermediates in a dissociation of PPh_3 in **1a–e**. The free energies for the 16-electron intermediate that results from PPh_3 dissociation from **1a–e** (second column in Table 5) are quite similar to each other and lower than the energies for intermediates resulting from halide dissociation and coordination of THF (third column in Table 5). The calculated free energy changes for the overall conversion of **1a–e** to **2a–e** are listed in the fourth column of Table 5 indicating a fairly narrow range of value for ΔG of about 12 kJ mol^{-1}.

 This journal is © The Royal Society of Chemistry 2017

Open Access Article. Published on 07 July 2017. Downloaded on 2/5/2026 2:55:27 PM.
This article is licensed under a Creative Commons Attribution 3.0 Unported Licence.

Table 3 Estimated first order rate constants for substitution of PPh_3 by $PMePh_2$ in **1a–e** in $CDCl_3$[a] and first order rate constants for the reaction of **1c–d** with $CDCl_3$

X	$k_{30,susb,CDCl_3}$ ($\times 10^6$ s^{-1})	$k_{30,THF}/k_{30,susb,CDCl_3}$	$k_{30,CDCl_3}$ ($\times 10^6$ s^{-1})	$k_{30,susb,CDCl_3}/k_{30,CDCl_3}$
1a, Cl	13[b]	2.2[b]	—	—
1b, Br	5.0 ± 0.3	1.6		—
1c, I	1.8 ± 0.2	1.4	0.54 ± 0.2	3
1d, N_3	6.1 ± 0.1	4.0	6.6 ± 0.4	1
1e, NCO	3.5 ± 0.5	4.6	—	—

[a] Concentrations of **1a–e** ranged from 12 to 18 mM in $CDCl_3$ with $a \approx 10$ fold excess of $PMePh_2$. [b] From data in ref. 6 and 7.

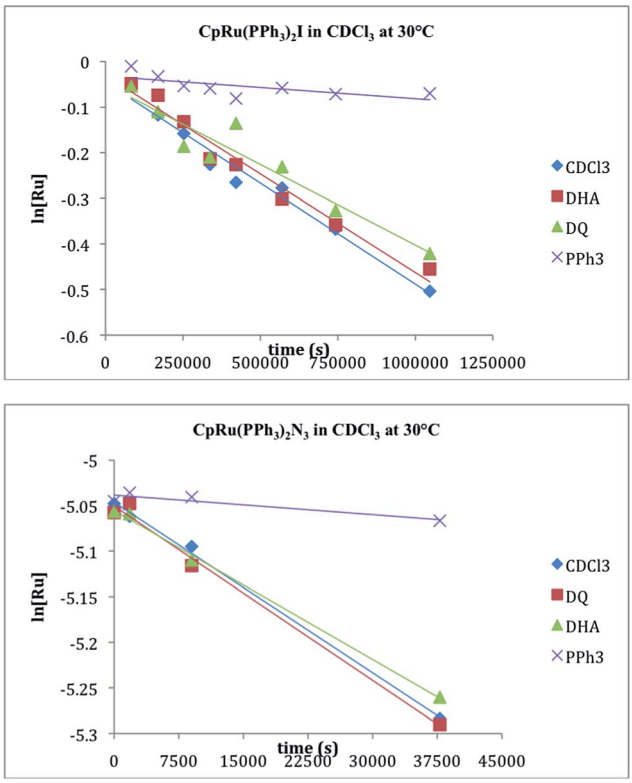

Fig. 3 Plot of ln[$CpRu(PPh_3)_2I$] *vs.* time (s) for halide exchange in $CDCl_3$ solution at 30 °C. (a) **1c** in the presence of 9,10-dihydroanthracene (DHA, 3 eq.), duroquinone (DQ, 7 eq.) and PPh_3 (21 eq.) and (b) **1d** in the presence of 9,10-dihydroanthracene (DHA, 2 eq.), duroquinone (DQ, 3 eq.) and PPh_3 (6 eq.).

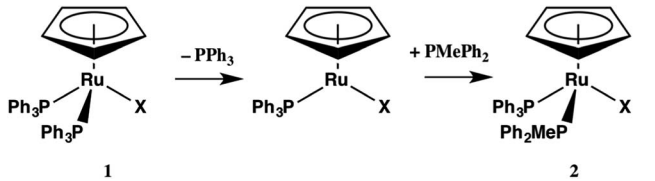

(2)

The energies of the transition states for the two steps in eqn (2) were also calculated (Table 6). The data indicate that the activation energy for the dissociation of PPh_3 is greater than for the reaction of the 16 e^- intermediate, $CpRu(PPh_3)X$, with $PMePh_2$, consistent with the kinetic measurements. The calculated values of ΔG for the transitions states of **1a–e** are also quite close in energy, covering a range of <4 kJ mol^{-1} for the rate-determining step and about 8–12 kJ mol^{-1} less than the values of $\Delta G^{\ddagger}$ from experiment.

Discussion

The effect of the X group on phosphine substitution rates in **1a–e** is qualitatively similar to those reported previously for $Cp^*Ru(PMe_3)_2X$ for the same set of X ligands. An increase in the rate of substitution in $Cp^*Ru(PMe_3)_2X$ is observed for X ligands with lone pairs of electrons on the donor atom, *e.g.* X = Cl, Br, I, NPh_2, NHPh, OPh, OH, and SH relative to such σ-donor ligands such as H, CH_3, CH_2Ph, Ph and CH_2SiMe_3.[9] Kinetic data for phosphine exchange between $Cp^*Ru(PMe_3)_2X$ and PMe_3 in aromatic hydrocarbon solution are consistent with

Table 4 Calculated[a] and observed[b] bond distances and bond angles for **1a–e**

Compound	d_{Ru-X} (Å)	d_{Ru-P1} (Å)	d_{Ru-P2} (Å)	$d_{Ru-Cp,centroid}$ (Å)	$\angle_{Ru-X}$ (°)
1a	2.513	2.401	2.396	2.27	—
	2.448[b]	2.323[b]	2.329[b]	2.20[b]	—
1b	2.648	2.406	2.411	2.27	—
	2.568[b]	2.323[b]	2.329[b]	2.214[b]	—
1c	2.842	2.416	2.413	2.275	—
1d	2.196	2.401	2.400	2.275	118.5
	2.135[b]	2.329[b]	2.330[b]	1.843[b]	124.5[b]
1e	2.136	2.400	2.3999	2.27	153.5

[a] The isocyanate ligand is treated as N bonded. Calculations use the B3LYP functional and the DGDZVP basis set on the Gaussian 09 suite. Normal convergence conditions were applied and geometries were determined to be of a minimal through a frequency calculation. [b] From X-ray crystallography see ref. 19. This value seems abnormally short for a Cp–Ru bond.

Open Access Article. Published on 07 July 2017. Downloaded on 2/5/2026 2:55:27 PM.
This article is licensed under a Creative Commons Attribution 3.0 Unported Licence.

Table 5 Calculated Gibbs free energies (kJ mol^{-1}) for PPh_3 dissociation, halide dissociation and the overall phosphine substitution reactions of **1a–e**[a]

	ΔG (kJ mol^{-1})	ΔG (kJ mol^{-1})	ΔG (kJ mol^{-1})
$CpRu(PPh_3)_2X$	$CpRu(PPh_3)_2X \Rightarrow CpRu(PPh_3)X + PPh_3$	$CpRu(PPh_3)_2X + THF \Rightarrow CpRu(PPh_3)_2(THF)^+ + X^-$	$CpRu(PPh_3)_2X + PMePh_2 \Rightarrow CpRu(PMePh_2)(PPh_3)X + PPh_3$
1a, X = Cl	43.5	70.9	−35.8
1b, X = Br	40.7	59.0	−40.8
1c, X = I	43.6	47.2	−45.2
1d, X = N_3	47.2	105.1	−32.6
1e, X = NCO	43.9	108.8	−31.9

[a] Geometry optimizations were optimized in the gas phase using the B3LYP exchange–correlation functional and DGDZVP basis set followed by a single point energy calculation using a polarizable continuum model (PCM) for THF solvation.

Table 6 Calculated Gibbs free energies (kJ mol^{-1}) for transition states for PPh_3 dissociation and the subsequent phosphine substitution reactions of **1a–e**[a]

	$\Delta G^{\ddagger}_{TS1}$ (kJ mol^{-1})	$\Delta G^{\ddagger}_{TS2}$ (kJ mol^{-1})
$CpRu(PPh_3)_2X$	$CpRu(PPh_3)_2X \Rightarrow [CpRu(PPh_3)X\cdots PPh_3]^{\ddagger}$	$CpRu(PPh_3)_2X + PMePh_2 \Rightarrow [CpRu(PMePh_2)(PPh_3)X]^{\ddagger}$
1a, X = Cl	92.1	73.7
1b, X = Br	93.2	75.7
1c, X = I	91.1	80.0
1d, X = N_3	89.6	79.9
1e, X = NCO	91.1	79.5

[a] The transition state optimization was performed using the synchronous transit and quasi-Newton methods (STQN). The guess structure used was the maximum of a relaxed PES scan along the Ru–P bond. They were confirmed as first order saddle points by harmonic frequency analysis.

a dissociative process through 16-electron $Cp^*Ru(PMe_3)X$ intermediates.[9] The relative rates of substitution in $Cp^*Ru(PMe_3)_2X$ were judged to reflect both ground state and transition state effects of X.[9] The observation that **1g–i** (X = H, SnF_3, and $SnCl_3$) do not react at all with $PMePh_2$ under the reaction conditions is consistent with the observations for $Cp^*Ru(PMe_3)_2X$: good σ-donors lead to slower reaction. The corresponding indenyl complex, $(\eta^5\text{-}C_9H_7)Ru(PPh_3)_2H$, is also known to be inert toward phosphine substitution.[20] The effect of σ-donor, π-donor, and possibly π-acceptor properties of the ligands on both ground state and transition state energies are likely to be relevant to interpretations of the rate data for **1a–e**.

We start by considering the halide derivatives **1a–c**. The observed order of substitution rates in **1a–c** are the same as for $Cp^*Ru(PMe_3)_2X$: Cl > Br > I. The substitution rates in **1a–c** span a relatively small range; k_{obs} for **1a** (X = Cl) is ≈ 50 times greater than for **1c** (X = I) in THF, a slightly broader range of k_{obs} values for **1a–c** than for $Cp^*Ru(PMe_3)_2X$ for the same X ligands. A dissociative mechanism for phosphine substitution has been suggested for reactions of **1a** with $PMePh_2$ in both THF and $CDCl_3$.[6,7] The kinetic data for substitution in **1b** and **1c** in Table 1 in THF are also consistent with a dissociative or dissociative interchange mechanism with the loss of PPh_3 as the rate-determining step.[6] This conclusion is supported by the observed decrease in rate in the presence of added PPh_3, the independence of the rate on $PMePh_2$ concentration and the observed positive activation entropies. Closer examination of the effect of added PPh_3 on the substitution rate reveals that the effect is not the same across the series **1b–e**.

Ionization of Ru–X bonds in $CpRu(PR_2R')_2X$ (R = Ph, Me, X = Cl, Br, I) systems in Lewis basic solvents such as alcohols, acetonitrile, or dimethylsulfoxide is well established but does not seem to play a significant role in the substitution reactions in THF.[21] The absence of any significant effect of added X^- on the rate suggests that formation of $[CpRu(PPh_3)_2(THF)]^+$ and X^- ions in THF solution is unlikely to be the rate determining step; one would expect a decrease in rate if dissociation of X^- was the rate determining step. With the exception of **1c** calculations of the relative energies of $CpRu(PPh_3)X$ and $[CpRu(PPh_3)_2(\text{-}THF)]^+[X]^-$ confirm that the latter is significantly higher in energy than the former. Even in the case of $CpRu(PPh_3)_2I$ (**1c**), the 16 e$^-$ intermediate is 3–4 kJ mol^{-1} lower in energy than $[CpRu(PPh_3)_2(THF)]^+[I]^-$ (in the gas phase).

The absence of significant differences in the Ru–P or Ru–Cp bond distances in **1a–c** in either the crystal structures or in the calculated structures (Table 4) suggests that only small differences exist in the ground state energies of **1a–c**. Despite a significantly larger ionic radius and a longer Ru–X bond distance, the iodide (**1c**), reacts slower than the chloride (**1a**). Increasing the size of X (X = I > Br > Cl) does not increase the

 This journal is © The Royal Society of Chemistry 2017

Open Access Article. Published on 07 July 2017. Downloaded on 2/5/2026 2:55:27 PM.
This article is licensed under a Creative Commons Attribution 3.0 Unported Licence.

rate of the reaction suggesting that transition state effects also contribute to the order of substitution rates for **1a–c**.[9,22] The electrochemical potentials of $CpRu(PPh_3)_2X$ (Table 1) reveal surprisingly similar E° values for **1a–c**. The E° values for **1a–c** are essentially indistinguishable: 136 *vs.* 138 mV *vs.* Fc/Fc^+ for **1a** and **1b**, respectively and less than a 50 mV difference in E° between the chloride and iodide complexes. Although **1c** does react slower than **1a–b**, the small difference in E° values remains consistent with minimal contribution from ground state effects to the substitution reaction. Further support for small ground state effects of chloride, bromide and iodide is seen in the ν_{CO} for $CpRu(CO)_2X$ (ν_{CO} X = Cl > Br > I) which differ by only 11 cm^{-1}.[23]

Interestingly $CpRu(PPh_3)_2F$ (**1f**) has a significantly larger positive E°, 790 mV, which may help explain the lack of reactivity toward $PMePh_2$. Fluoride is a weaker σ-donor and a stronger π-donor than Cl^-, Br^- and I^-.[2] One not on might expect greater π-donation to accelerate the substitution rate but the opposite is observed. The much greater electronegativity of fluoride as reflected by E°, suggests that the Ru–PPh_3 bond is significantly stronger in **1f** than in **1a–c** contributing to the failure of $CpRu(PPh_3)_2F$ (**1f**) to react with $PMePh_2$ under the conditions of the experiment. No data is available for $Cp^*Ru(PMe_3)_2F$ for $CpRu(CO)_2F$ making further comparisons difficult.

The calculated free energies of the 16-electron $CpRu(PPh_3)X$ fragments span a narrow range, about 10 kJ mol^{-1} (Table 5). It was previously shown that PPh_3 dissociation from **1a** yields a lower energy intermediate than dissociation of Cl^- to form $CpRu(PPh_3)_2^+$, the common intermediate from halide dissociation from **1a–c**.[6] The computational results for the free energies of the $CpRu(PPh_3)X$ intermediate must be treated with caution when comparing calculations in the gas phase to the kinetic measurements in solution. As expected, the calculated free energy changes for substitution of one PPh_3 by $PMePh_2$ for the halide compounds are exergonic ($\Delta G < 0$, Table 5) and differ by <15 kJ mol^{-1} as a function of the halide ligand.

Support for the role of transition state effects on the reactivity of **1a–c** comes from decades-old studies of carbonyl substitution reactions of $M(CO)_5X$ (M = Re, Mn) and $M(CO)_5X^-$ (M = Cr, Mo, where X = Cl, Br and I).[24] Substitution *cis* to the X group is observed in all cases and kinetic data for these reactions are consistent with a dissociative pathway. The rate of substitution in the chloride complexes is between 15 and 250 times the rate of substitution in the corresponding iodides. This effect was attributed to stabilization of the 16-electron intermediate or transition state by the stronger σ-donation from the halide ligand: Cl > Br > I.[24] There are strong parallels between the substitution rates in these mononuclear metal carbonyl halides and **1a–c**. The observed order of rates, Cl > Br > I, is the same and substitution in **1a–c** also occurs *cis* to the X group if one considers the Cp ligand to occupy a *fac* geometry in a pseudo-octahedral geometry. A stabilizing role for π-donation from X is less likely because the order of π-donation, I > Br > Cl, does not match the relative rates of phosphine substitution.[1,22] The kinetics of carbonyl substitution in $CpRu(CO)_2X$ provide an even better comparison with the reactions of **1a–c**.[25] In xylene, the rate of substitution in $CpRu(CO)_2Cl$ with $P(OPh)_3$ is faster than for the bromide and iodide. A dissociative process is proposed for all three $CpRu(CO)_2X$ compounds.

Finally, the calculated transition state energies ($\Delta G^\ddagger$) for the reactions of **1a–c** with $PMePh_2$ support the interpretation of the experimental data. The first step, dissociation of PPh_3, is the rate determining step with subsequent reaction of the coordinatively unsaturated $CpRu(PPh_3)X$ intermediate with $PMePh_2$: $\Delta G^\ddagger_{TS1} > \Delta G^\ddagger_{TS2}$. The difference between $\Delta G^\ddagger_{TS1}$ and $\Delta G^\ddagger$ (Table 2) is small. The range of values for $\Delta G^\ddagger_{TS1}$ is quite narrow and mirrors the trend for $\Delta G^\ddagger$ in Table 2 suggesting that only small differences in the transition state contribute to the observed order of reaction rates: **1a** > **1b** > **1c**. For **1c**, the similar energies for two intermediates, $CpRu(PPh_3)I$ and $[CpRu(PPh_3)_2(THF)]^+[I]^-$ in Table 5 may account for the greater difference between $\Delta G^\ddagger_{TS1}$ and $\Delta G^\ddagger$.

The compounds with pseudohalide ligands (N_3^- and NCO^-), **1d** and **1e**, introduce ligands with both π-donating and π-accepting properties. Compounds **1d** and **e** react with $PMePh_2$ as fast, or even faster, than **1b**. Unlike **1a–c**, the activation entropies for **1d** and **1e** are negative: $\Delta S^\ddagger = -48 \pm 16$ and -105 ± 23 J mol^{-1} K^{-1}, respectively. This raises the possibility of a change in mechanism from a dissociative interchange to an associative interchange pathway. Nevertheless, the observation that the substitution rate in both **1d** and **1e** decreases in the presence of excess PPh_3 and is unchanged when excess pseudohalide is added to the solution argues for a dissociative or dissociative interchange mechanism for **1a–e**. The greatest effect of added PPh_3 on rate is seen for **1d**, the compound that reacts the fastest and the smallest effect is seen for **1c**, which exhibits the slowest rate of phosphine substitution. One possible explanation is that the halide complexes, **1b–c** react by a dissociative interchange mechanism while substitution in **1d–e** follows a more dissociative pathway.

If ionization of the pseudohalide ligand in **1d–e** represents the rate determining step, then one expects a decrease in rate when excess N_3^- or NCO^- is added to the reaction mixture, yet the rate is unchanged. Calculated values of ΔG for product of substitution of N_3^- or NCO^- by THF, $[CpRu(PPh_3)_2(THF)]^+[X]^-$, are more than double the ΔG for $CpRu(PPh_3)X$, suggesting that dissociation of X^- also does not play a role in the reaction with $PMePh_2$. Large negative values for $\Delta S^\ddagger$ were also reported for phosphine substitution in (η^5-pentadienyl)$Ru(PPh_3)_2Cl$ in what appears to be a dissociative mechanism and have been observed in halide exchange reactions of CpRu(prophos)Cl.[26] The large positive $\Delta S^\ddagger$ values for substitution in $Cp^*Ru(PMe_3)_2X$ were attributed to a late or product like transition state[9] so one possible explanation for the differences in $\Delta S^\ddagger$ values between **1a–c** and **1d–e** is an earlier, more ordered transition state in **1d–e** than in **1a–c**. For comparison, the activation entropy for substitution in $Re(CO)_5NCO$, $\Delta S^\ddagger = +8$ J mol^{-1} K^{-1}, is less positive than $\Delta S^\ddagger = +73$ and $+44$ J mol^{-1} K^{-1} for substitution in $Re(CO)_5Cl$ and $Re(CO)_5Br$, respectively.[27] The rate of substitution in the rhenium(I) series reveals that $Re(CO)_5NCO$ reacts slightly slower than $Re(CO)_5Cl$ but faster than the bromide derivative similar to our observations for **1a–b** and **1e**.[27] Detailed calculations of the structure of the transition state for **1a–e** are

Open Access Article. Published on 07 July 2017. Downloaded on 2/5/2026 2:55:27 PM.
This article is licensed under a Creative Commons Attribution 3.0 Unported Licence.

in progress but the data for $\Delta G^{\ddagger}_{TS1}$ indicate a lower activation energy for **1d** and correlate well with the values for $\Delta G^{\ddagger}$ in Table 2, as observed for **1a–c**.

The Ru–P bond distances in the solid state structure of **1d**[19c] and the results of DFT calculations (Tables 4 and 5) for **1d–1e** do not reveal any striking structural anomalies. The electrochemical potential for **1e** is again indistinguishable from the values for **1a–1c** suggesting similar ground state energies. The electrochemistry of **1d**, however, indicates that it is much easier to oxidize than **1a** or **1b** by about 160 mV. The significance of this E° value on the relative value of k_{obs} is not entirely clear but may indicate a slightly higher energy for the ground state in **1d**.

Crystallography confirms that the azide ligand in **1d** is bent with a Ru–N–N bond angle of 124.5°.[19c] DFT calculations are consistent with this geometry yielding a calculated bond angle, $\angle_{Ru-N-N} = 118.5°$. The calculated Ru–N–C bond angle in **1e** (153.5°) reveals that the NCO ligand is more linear in **1e**, consistent with a greater contribution of resonance forms **C** and **D** in Fig. 4, while structures **A** and **B** are likely to be the major contributors to the bonding of N_3^- in **1d**. The importance of structures **C** and **D** may make the linear NCO ligand a better π-acceptor than the bent N_3 ligand.

Transition state stabilization and increased substitution rates for square planar complexes bearing ancillary π-acceptor ligands is well established but the effect of π-acceptor ligands on substitution rates in octahedral complexes is less documented.[22] Seminal studies on dissociative substitution reactions of group 6 and group 7 carbonyls suggest that 16 e^- transition states are stabilized by electron donors and destabilized by acceptor ligands.[22,24,27] If this is true, than the bent N_3 ligand in **1d** stabilizes the transition state and accounts for the faster reaction of **1d** compared to **1e**. Conversely, the better π-acceptor, linear NCO ligand may destabilize (raise the energy of) the transition state decreasing the reaction rate. The linear π-accepting phenylacetylide ligand in $Cp^*Ru(PMe_3)_2CCPh$ increases the Ru–PMe_3 bond energy by about 38 kJ mol^{-1} and reduces the rate of phosphine dissociation.[9] Significantly slower phosphine substitution was also observed in reactions of $(\eta^5\text{-}C_9H_7)Ru(PPh_3)_2CCPh$ compared to $(\eta^5\text{-}C_9H_7)Ru(PPh_3)_2Cl$.[20]

In addition to **1f**, phosphine substitution was also not observed in **1g–i** all of which contain good σ-donors: hydride and trihalotin (SnX_3^-, X = Cl, F) ligands. To understand the lack of reaction, we turn to the studies of phosphine substitution that include $Cp^*Ru(PMe_3)_2Cl$, $Cp^*Ru(PMe_3)_2H$, and $Cp^*Ru(PMe_3)_2CH_3$.[9] The data for the latter three compounds suggests that the activation enthalpy, $\Delta H^{\ddagger}$, for the reaction closely approximates the Ru–PMe_3 bond energies, leading to the conclusion that the Ru–PMe_3 bonds in $Cp^*Ru(PMe_3)_2H$ and $Cp^*Ru(PMe_3)_2CH_3$ are 29–59 kcal mol^{-1} greater than for $Cp^*Ru(PMe_3)_2Cl$. The lack of phosphine substitution in **1g–i** is therefore, most likely the result of a small, strong σ-donor hydride ligands that substantially greater Ru–P bond strength.

The observation of halide exchange reactions between $CpRu(PPh_3)_2X$ and $CDCl_3$ has not been previously reported[28] for **1b–e** although reaction between **1a** and acetyl halides, CH_3COX where X = Br and I, was recently reported to yield **1b–c**.[29] An increase in the rate of halide exchange was observed in the presence of 9,10-dihydroanthracene (radical initiator) and a concomitant decrease in conversion when TEMPO (radical trap) is added to the reaction mixture supporting a radical mechanism. Computational chemistry suggested a pathway where phosphine dissociation is followed by halogen atom abstraction from CH_3COX and formation of a radical pair.[29] Further support for radical intermediates in the chemistry of **1** is found in the catalytic activity of $CpRu(PPh_3)(PMe_3)Cl$ in the atom transfer radical addition (ATRA) reactions of CCl_4 and styrene.[30] There are also two reports of the reaction between **1a** and excess iodomethane yielding **1c** *in situ* and as a synthetic method but the mechanism of the reaction was not explored.[3]

The reactions between **1c–d** and $CDCl_3$, however, are inconsistent with radical mechanisms given the absence of any noticeable effect of 1–16 equivalents of 9,10-dihydroanthracene or duroquinone (Fig. 3).[25a] The addition of PPh_3 significantly reduces the rate of the halide exchange reaction. The latter observation argues for phosphine substitution as the potential rate-limiting step in the halide exchange reaction. The relative rates of halide exchange for **1c** and **1d** mimic the trend for the phosphine substitution rates in these two compounds. Both the oxidative addition of C-halide bonds and concerted mechanisms (Fig. 5) must be considered for the conversion of **1c–d** to **1a**.

Limited evidence for both mechanisms can be found in the literature. Oxidative addition of allyl chloride to $CpRu(PPh_3)_2Cl$ yields $CpRu(C_3H_5)Cl_2$ (ref. 31) while a halocarbon complex, $[CpRu(PPh_3)_2(CH_3I)][PF_6]$ is isolated from reaction of **1a** with Ag^+ and methyl iodide.[32] A further mechanistic proposal for the halide exchange reaction is the formation of quaternary phosphonium salts by reaction between the dissociated PPh_3 and $CDCl_3$ followed by dissociation of Cl^- and subsequent halide exchange with **1b–e**. The latter pathway was proposed for the *catalytic* halogen exchange between MeI and CH_2Cl_2 catalyzed by a broad range of group 9 transition metal complexes.[33] Although no new resonances are observed in the ^{31}P NMR spectrum of PPh_3 in $CDCl_3$, the possibility of halide exchange in **1b–e** by this mechanism cannot be excluded at this time.

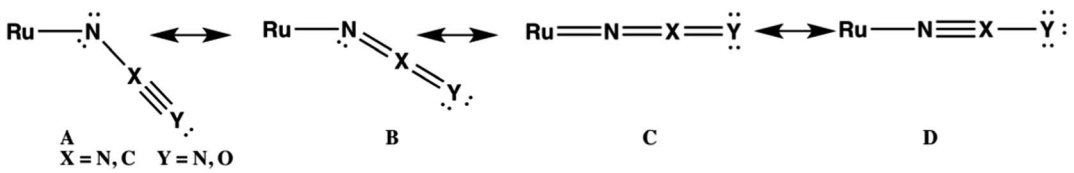

Fig. 4 Resonance forms for the pseudohalide ligands in **1d–e**.

 This journal is © The Royal Society of Chemistry 2017

Open Access Article. Published on 07 July 2017. Downloaded on 2/5/2026 2:55:27 PM.
This article is licensed under a Creative Commons Attribution 3.0 Unported Licence.

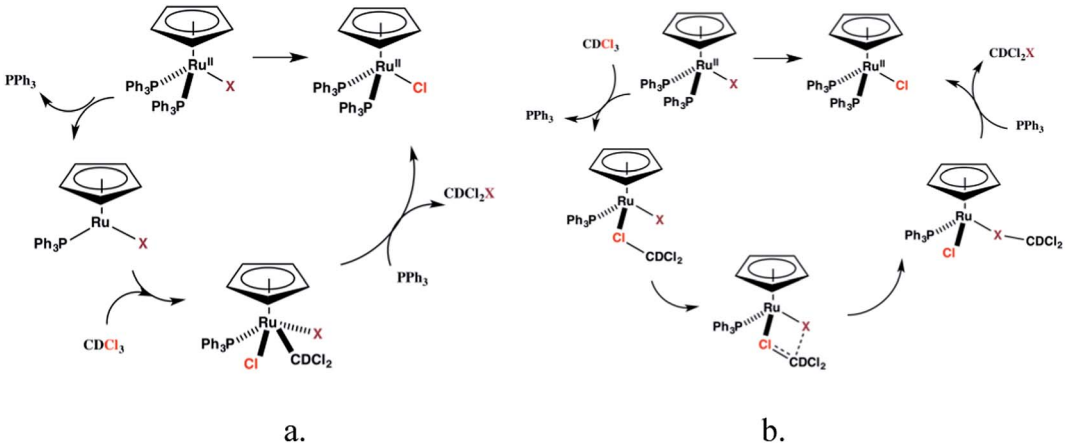

Fig. 5 Possible mechanisms for halide exchange in **1c–d**.

The rate data for phosphine substitution in **1a–i** provide some insight into reaction mechanisms where **1a–i** show catalytic activity. The assertion that faster phosphine dissociation accounts for higher yields in the cycloaddition of norbornene and norbornadiene[3] when **1c** is used in place of **1a** is inconsistent with the relative rates of phosphine substitution reported herein. In fact, our data suggest that any catalytic process that relies on phosphine dissociation from **1a–e** should proceed fastest for X = Cl with X = N_3 as the next most active catalyst precursor. The effect of **1b–e** on the rate and selectivity of ruthenium-catalyzed dimerization of alkynes[34] and the 1,3-dipolar addition of azides to alkynes[35] represent potential future studies of the effect of the X ligand on catalytic properties. Phosphine substitution in trihalotin ligands in **1h–i** are clearly slow and consistent with the high temperatures required for converting methanol to methylacetate[5] in their presence.

Conclusions

The results of the kinetic study of phosphine substitution in $CpRu(PPh_3)_2X$ for five halide and pseudohalide derivatives in THF and $CDCl_3$ solution reveals a likely dissociative or dissociative interchange process. These data suggest that dissociative substitution mechanisms reported for $CpRu(PAr_3)_2Cl$[6] and $Cp^*Ru(PMe_3)_2X$ complexes[9] are a general reaction pathway for 18-electron, cyclopentadienyl ruthenium(II) derivatives. Differences in the rate of substitution in **1a–e** are likely a combination of ground state and transition state effects. Dissociation of phosphine in **1b–e** is a likely step in the exchange of Ru–X bonds for Ru–Cl bonds when $CpRu(PPh_3)_2X$ is dissolved in $CDCl_3$, however, further mechanistic studies are needed to identify the likely mechanism.

For reactions where Ru–X bond ionization is important, the data on phosphine substitution in **1a–e** offer more limited insight. Compounds **1a**, **1c–d**, **1g** and **1i** all catalyze the *N*-methylation of cyclohexylamines[4] to varying degrees in methanol solution. An order of relative rates, **1a** > **1g** > **1c** ≥ **1d** ≫ **1i** (no reaction), can be inferred from the observed product ratios of $CyNMe_2$: CyNHMe : $CyNH_2$. Among these, **1a** is by far the best catalyst but the position of the hydride complex, **1g**, is anomalous suggesting that more work is needed to understand the effect of different ligand environments on the reactivity of cyclopentadienyl ruthenium(II) complexes in carbon–carbon and carbon–nitrogen bond forming processes.

References

1 *Ruthenium in Organic Synthesis*, ed. S.-I. Murahashi, Wiley-VCH, 2004.
2 For a review of halide effect in transition metal catalyzed reactions see K. Fagnou and M. Lautens, *Angew. Chem., Int. Ed.*, 2002, **41**, 26–47.
3 (*a*) A. Tenaglia and L. Giordano, *Synlett*, 2003, 2333–2336; (*b*) A. Tenaglia and M. Sylvain, *J. Org. Chem.*, 2008, **73**, 1397–1402; (*c*) A. Tenaglia, L. Giordano, M. Sylvain and I. De Riggi, *Angew. Chem. Int. Ed.*, 2011, **50**, 9062–9065.
4 A. Del Zotto, W. Baratta, M. Sandri, G. Verardo and P. Rigo, *Eur. J. Inorg. Chem.*, 2004, 524–529.
5 P. A. Robles-Dutenhefner, E. M. Mora, G. J. Gama, H. G. L. Siebald and E. V. Gusevskaya, *J. Mol. Catal. A: Chem.*, 2000, **164**, 39–47.
6 (*a*) M. J. Verschoor-Kirss, O. Hendricks, L. Renna, D. Hill and R. U. Kirss, *Dalton Trans.*, 2014, **43**, 15221–15227; (*b*) C. Peng and H. B. Schlegel, *Isr. J. Chem.*, 1993, **33**, 449.
7 M. P. Gamasa, J. Gimeno, C. Gonzalz-Bernardo, B. M. Martin-Vaca, D. Monti and M. Bassetti, *Organometallics*, 1996, **15**, 302–308.
8 (*a*) R. J. Haines and A. L. DuPreez, *J. Organomet. Chem.*, 1975, **84**, 357–367; (*b*) P. M. Treichel and P. J. Vincenti, *Inorg. Chem.*, 1985, **24**, 228–230.
9 H. E. Bryndza, P. J. Domaille, R. A. Paciello and J. E. Bercaw, *Organometallics*, 1989, **8**, 379–385.
10 D. F. Shriver, *Manipulation of Air Sensitive Compounds*, McGraw Hill, 1969.
11 M. I. Bruce, C. Hameister, A. G. Swincer and R. C. Wallis, *Inorg. Synth.*, 1990, **28**, 270.
12 T. Wilczewski, M. Bochenska and J. F. Biernat, *J. Organomet. Chem.*, 1981, **215**, 87–96.

Open Access Article. Published on 07 July 2017. Downloaded on 2/5/2026 2:55:27 PM.
This article is licensed under a Creative Commons Attribution 3.0 Unported Licence.

13 E. M. Moura, H. G. L. Siebald and G. M. de Lima, *Polyhedron*, 2002, **21**, 2323–2331.
14 (*a*) M. I. Bruce, C. Hameister, A. G. Swincer and R. C. Wallis, *Inorg. Synth.*, 1982, **21**, 78–84; (*b*) M. I. Bruce, R. C. F. Gardner and F. G. A. Stone, *J. Chem. Soc., Dalton Trans.*, 1976, 81–89.
15 P. M. Treichel and D. A. Komar, *Synth. React. Inorg. Met.-Org. Chem.*, 1980, **10**, 205–218.
16 G. Lente, I. Fabian and A. J. Poe, *New J. Chem.*, 2005, **29**, 759–760.
17 D. A. Skoog, D. M. West and J. Holler, *Analytical Chemistry: An Introduction*, Saunders, 7th edn, 2000.
18 See ESI† for plots of ln[Ru] *vs.* time, complete tables of rate constants and Eyring plots for reactions of **1b–e** with $PMePh_2$.
19 (*a*) M. I. Bruce, F. S. Wong, B. W. Skelton and A. H. White, *J. Chem. Soc., Dalton Trans.*, 1981, 1398–1405; (*b*) M. I. Bruce, P. J. Low, B. W. Skelton, E. R. T. Tietink, A. Werth and A. H. White, *Aust. J. Chem.*, 1995, **48**, 1887–1892; (*c*) M. M. T. Khan, M. M. Bhadbhade, M. R. H. Siddiqui and K. Venkatasubramanian, *Acta Crystallogr., Sect. C: Cryst. Struct. Commun.*, 1994, **50**, 502–504.
20 M. Bassetti, S. Marini, F. Tortorella, V. Cadierno, J. Diez, M. P. Gamasa and J. Gimeno, *J. Organomet. Chem.*, 2000, **593–594**, 292–298.
21 Rate constants for solvation for $CpRu(PPh_2OMe)_2X$ and $CpRu(PPh_2Me)_2X$ in CD_3CN comparable to the substitution rates for $CpRu(PPh_3)_2X$ at 30 °C require more than doubling the reaction temperature to 67 °C. Compound **1a–c** do not dissolve sufficiently in CD_3CN for a direct comparison. See ref. 8.
22 J. M. Atwood, *Inorganic and Organometallic Reaction Mechanisms*, Wiley-VCH, 2nd edn, 1997.
23 R. J. Haines and A. L. duPreez, *J. Chem. Soc., Dalton Trans.*, 1972, 944–948.
24 J. D. Atwood and T. L. Brown, *J. Am. Chem. Soc.*, 1976, **98**, 3160–3166.
25 (*a*) K. Tabataiana and K. White, *Inorg. Chem.*, 1981, **20**, 2020–2022; (*b*) D. A. Brown, H. J. Lyons and R. T. Sane, *Inorg. Chim. Acta*, 1970, **4**, 621–625.
26 (*a*) M. Daniels and R. U. Kirss, *J. Organomet. Chem.*, 2007, **692**, 1716–1725; (*b*) H. Brunner, M. Muschiol, T. Tsuno, T. Takahashi and M. Zabel, *Organometallics*, 2008, **27**, 3514–3525.
27 R. J. Angelici and G. C. Faber, *Inorg. Chem.*, 1971, **10**, 514–517.
28 Halide exchange is also observed between **1c** and benzylbromide but not with bromobenzene.
29 H. Kuniyasu, A. Sanagawa, T. Nakajima, T. Iwasaki, N. Kambe, K. Bobuatong and M. Ehara, *J. Organomet. Chem.*, 2014, **769**, 34–39.
30 R. P. Nair, T. H. Kim and B. J. Frost, *Organometallics*, 2009, **28**, 4681–4688.
31 H. Nagashima, K. Mukai, Y. Shiota, K. Yamaguchi, K.-I. Ara, T. Fukahori, H. Suzuki, M. Akita, Y. Moro-oka and K. Itoh, *Organometallics*, 1990, **9**, 799–807.
32 (*a*) R. J. Kulawiec, J. W. Faller and R. H. Crabtree, *Organometallics*, 1990, **9**, 745–755; (*b*) A related complex, $[CpRu(PPh_3)(CN^tBu)(CH_3I)]^+$ is also known: F. M. Conroy-Lewis, A. D. Redhouse and S. J. Simpson, *J. Organomet. Chem.*, 1989, **366**, 357–367.
33 D. Forster, *J. Chem. Soc., Chem. Commun.*, 1975, 917–918.
34 M. Daniels and R. U. Kirss, *J. Organomet. Chem.*, 2007, **692**, 1716–1725.
35 L. Zhang, X. Cheng, P. Xue, H. H. Y. Sun, I. D. Williams, K. B. Sharpless, V. V. Fokin and G. Jia, *J. Am. Chem. Soc.*, 2005, **127**, 15998–15999.

This journal is © The Royal Society of Chemistry 2017